Available online at www.sciencedirect.com

SciVerse ScienceDirect

Ceramics International 39 (2013) 3183–3188

CERAMICS INTERNATIONAL

www.elsevier.com/locate/ceramint

Synthesis of hexagonal $YMnO_3$ from precursor obtained by the glycine–nitrate process

Aboalqasim Alqat[a,*], Zohra Gebrel[a], Vladan Kusigerski[a], Vojislav Spasojevic[a], Marian Mihalik[b], Matus Mihalik[b], Jovan Blanusa[a]

[a]*The Vinca Institute, University of Belgrade, POB 522, 11001 Belgrade, Serbia*
[b]*Institute of Experimental Physics, Slovak Academy of Sciences, 04001 Kosice, Slovak Republic*

Received 13 September 2012; received in revised form 1 October 2012; accepted 2 October 2012
Available online 9 October 2012

Abstract

A new synthesis route for obtaining a single-phase hexagonal $YMnO_3$ was developed, based on the annealing of the amorphous precursor powder obtained by the glycine–nitrate combustion method. The process was monitored by XRD as well as by magnetic and heat capacity measurements. The analysis of these data shows that precursor powder undergoes a gradual phase transformation that depends on the annealing temperature. The metastable orthorhombic $YMnO_3$ phase is the first to appear at temperatures below 700 °C, while a mixture of ortho- and hexa-phases was found to exist within the 700–900 °C range. An almost complete conversion to hexa-phase occurs at 900–1000 °C, but to obtain the pure, well crystallized h-$YMnO_3$ phase an annealing temperature of 1300 °C was necessary. The synthesis method applied in this work has been proved to be more convenient for obtaining single-phase h-$YMnO_3$ than by a solid state reaction. In addition, it is capable of producing sample free of parasitic phases that are often present in specimens obtained by other synthesis methods.

Keywords: Chemical preparation; Magnetic properties; Manganites; Multiferroics

1. Introduction

Manganites with the general formula $RMnO_3$, where R denotes rare-earth cation, can be found within two crystal symmetries, both attracting vast interest from the viewpoint of a basic science as well as due to their huge application potentials. For a large cation radius (R = Lu-Tb subgroup), these compounds crystallize in a perovskite structure type, in the orthorhombic space group (SG) Pnma. When being hole-doped through the partial R^{3+} substitution by A^{2+} cation (A = Ca, Sr, Ba) they exhibit colossal magnetoresistivity (CMR), which is of a substantial importance for possible applications [1]. For a smaller cation radius (R = Ho–Lu, Y, Sc), a hexagonal structure with the SG $P6_3cm$ proves to be the most stable crystal phase [2], although by applying special synthesis techniques, an orthorhombic structure can also be realized within this group of compounds [3].

Both perovskite and hexagonal manganites can exhibit multiferroic properties, meaning that both ferroelectric and magnetic ordering can coexist in the same material. A coupling between these ordering parameters is of interest for electronic industry, since it allows control of either ferroelectric properties by a magnetic field, or magnetic properties by an electric field [4]. However, in a majority of manganites this magnetoelectric coupling is of a small intensity, thus limiting their application usability. Interest in hexagonal $YMnO_3$ has been largely intensified after a discovery of a considerable dielectric constant anomaly found in the vicinity of its Néel temperature T_N [5], which points to a strong magnetoelectric coupling in this material. Consequently, the crystal structure, electric and magnetic properties of $YMnO_3$ has been thoroughly studied. The temperature of its ferroelectric ordering is found to be $T_{FE} \approx 900$ K, which is by an order of magnitude higher than its Néel temperature $T_N \approx 70$ K [6]. The magnetic ordering that establishes below T_N is geometrically frustrated since anti-ferromagneticaly interacting Mn^{3+} ions occupy the quasi-two-dimensional triangular lattice [7].

*Corresponding author.
E-mail address: abelqat@yahoo.com (A. Alqat).

0272-8842/$ - see front matter © 2012 Elsevier Ltd and Techna Group S.r.l. All rights reserved.
http://dx.doi.org/10.1016/j.ceramint.2012.10.002

In contrast to the crystal structure data and transport properties, existing reports on magnetic properties of a hexagonal h-$YMnO_3$ are not consistent. One can roughly distinguish between the two types of reported magnetic behavior. Samples belonging to the first type undergo the anti-ferromagnetic transition at T_N between 60 and 70 K, which is confirmed by a number of neutron scattering and magnetic measurements [8], showing also the characteristics of a magnetically frustrated system [9]. This type of behavior has been recognized as a footprint of a single-phase polycrystalline h-$YMnO_3$. The second type of $YMnO_3$ magnetic behavior is also frequently reported and characterized by the peak in the zero-field-cooled (ZFC) magnetization curve at around 41 K [10]. Its origin seems to be rather unclear and it is, in general, ascribed to the presence of structure defects and/or impurities. Proposed explanations point to several possible reasons: a small presence of orthorhombic o-$YMnO_3$ phase [11,12] undetected by an XRD; a small amount of Mn_3O_4 impurity [7,13,14]; sub-stoichiometry of oxygen (i.e. h-$YMnO_{3-\delta}$ composition) [13]; a re-entrant spin-glass transition as in the case of Mn rich h-$YMnO_3$ [15]. Except for the presence of an o-$YMnO_3$ phase, the rest of the above listed causes are linked to the deviation from nominal oxygen concentration in h-$YMnO_3$ samples. Moreover, it was reported that, due to its higher oxygen content, YMn_2O_5 is more stable than h-$YMnO_3$ at low temperature [16,17]. Having in mind all of the above listed facts, the quest for an appropriate synthesis technique necessary for obtaining single-phase stoichiometric h-$YMnO_3$ is obviously of paramount importance.

A commonly employed technique for h-$YMnO_3$ preparation is a conventional solid state reaction in air [18–20]. Such approach requires high sintering temperature and a long heating time. In addition, the intermediate grindings that are necessary to eliminate parasitic phases additionally prolong and complicate the preparation process. Recently, an SPS (Spark Plasma Sintering) technique followed by the annealing at 1200 °C in air was used for obtaining h-YMnO3 [21]. Although this approach significantly reduces the number of necessary steps in a synthesis procedure, the existence of unresolved ferromagnetic peak at 40 K points to a presence of an unknown parasitic phase in the final $YMnO_3$ sample.

In this work, we are presenting the new preparation route for the synthesis of polycrystalline h-$YMnO_3$. The glycine–nitrate combustion method was employed for the preparation of a precursor, which was afterwards annealed at temperatures up to 1300 °C in an inert atmosphere (nitrogen flow). An evolution of the crystal structure and magnetic properties is reported, and the evidences on a single-phase h-$YMnO_3$ composition of the final specimen are provided. This recommends the applied method as the convenient one for preparation of a pure h-$YMnO_3$.

2. Experimental

The $YMnO_3$ samples were prepared by sintering of a precursor powder obtained by the glycine–nitrate combustion method. The starting mixture consisted of an aqueous solution of glycine, $Mn(NO_3)_2$ and $Y(NO_3)_3$ in the molar ratio 1:1:1. The prepared solution was stirred for 1 h at room temperature in order to achieve high homogeneity.

The so-obtained solution was heated on a hot plate while stirring, in order to evaporate the excess water. The remaining material was further kept at 200 °C until a spontaneous ignition occurred, resulting in a black powder residue after a short combustion process. Before annealing, the powder was pressed in pellets applying a pressure of 1 T/cm^2. The pellets were annealed under nitrogen flow for 2 h at different temperatures ranging from 600 to 1300 °C.

A phase composition of the obtained samples was examined by an X-ray powder diffraction (XRPD) performed on a Philips 1050 diffractometer, using Ni-filtered Cu-Kα radiation and a Bragg-Brentano focusing geometry. Magnetic measurements were done by utilizing a Superconducting Quantum Interference Device (SQUID) magnetometer (Quantum Design MPMS XL-5). The specific heat was measured on a Quantum Design PPMS device in different magnetic fields up to 5 T.

3. Results and discussion

3.1. X-ray diffraction

The powder X-ray diffraction patterns of the sample obtained by combustion as well as of the samples subsequently annealed at several temperatures in the 600–900 °C range are shown in Fig. 1. In the patterns corresponding to the as-prepared sample and the S600 sample, no diffraction maxima can be identified, which points to their amorphous nature. In the XRD pattern of the S700 sample, only those diffraction maxima belonging to the orthorhombic phase of $YMnO_3$ (space group Pnma, JCPD Card No. 56617) were visible. Thus, under the applied annealing conditions, the metastable orthorhombic phase

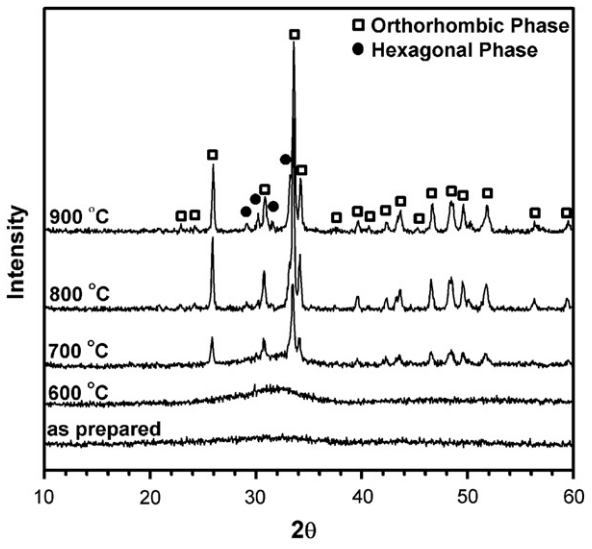

Fig. 1. Structural evolution of $YMnO_3$ powder as a function of annealing temperature.

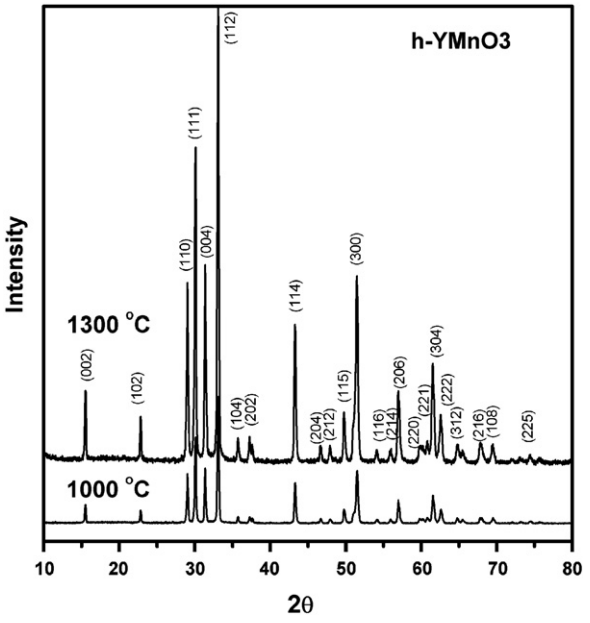

Fig. 2. XRD spectra of $YMnO_3$ annealed at 1000 °C and 1300 °C.

of $YMnO_3$ (marked by open squares in Fig. 1) is the first to crystallize at 700 °C. By increasing the annealing temperature up to 800 °C, additional peaks appeared (marked by filled circles), which correspond to a hexagonal $YMnO_3$ phase (SG $P6_3cm$, JCPD Card No. 154127). Subsequent annealing at 900 °C resulted only in a small increase of the hexagonal phase content.

XRD patterns of the samples annealed at temperatures above 900 °C are shown in Fig. 2. As it can be seen, an annealing for 2 h at 1000 °C resulted in a disappearance of the diffraction maxima belonging to the orthorhombic phase. Apparently, the complete conversion from the orthorhombic to the hexagonal phase in $YMnO_3$ occurs within the 900–1000 °C range. Increasing of the annealing temperature up to 1300 °C produced no visible changes in the diffraction pattern and, therefore, no visible change in the phase composition or the crystallinity of a sample. These results of an XRD analysis show that the applied synthesis method enables production of the hexagonal $YMnO_3$ sample already at annealing temperature of 1000 °C. The most common parasitic phases (Mn_3O_4, YMn_2O_5 and Y_2O_3) were not detected. However, it should be noted that due to proximity of the orthorhombic and hexagonal XRD spectra, as well as limited sensitivity of an XRD analysis, the X-ray data alone cannot serve as a definite evidence of a phase purity, as is clearly demonstrated by magnetic measurements described in Section 3.2.

3.2. Magnetic measurements

It is well known that high sensitivity magnetometry is an invaluable tool for probing the phase composition of magnetic materials, since it can detect a magnetic impurity phase even when its quantity falls far below the detection threshold of an XRD method. Two of the above listed impurity phases that can be found in $YMnO_3$ are magnetic (Mn_3O_4 – ferromagnetic ordering at $T_C \approx 42$ K [22], YMn_2O_5 – helical ordering at $T_C \approx 44$ K [23]), and in addition to these, an orthorhombic $YMnO_3$ also possesses anti-ferromagnetic ordering at $T_N = 41$ K [24,25]. Thus, in order to monitor the phase evolution during the synthesis process as well as phase purity of the obtained $YMnO_3$ samples, we have conducted the magnetic measurements on the SQUID-based magnetometer within the 2–100 K temperature range that encompasses the critical temperatures of the above listed magnetic phases.

Magnetization measurements were performed in two regimes: (i) in the zero-field-cooled (ZFC) regime where sample was cooled down to 2 K from the room temperature without magnetic field, and afterwards magnetization was recorded by heating the sample in the applied field, and (ii) in the field-cooled-regime (FC) in which sample was first cooled down in the applied field, and then its magnetization during heating in the same field was recorded. The ZFC and FC magnetization branches for S700 and S800 samples recorded in an applied magnetic field of 100 Oe are depicted in Fig. 3(a) and (b), respectively. Two maxima, centered at around 8 K and 42 K, can be observed in the ZFC branch of both samples. The peak at 42 K is identified as a critical point of the AF phase of ortho-$YMnO_3$. The peak at 8 K for S700 sample is narrow while the ZFC–FC bifurcation point is located at the peak

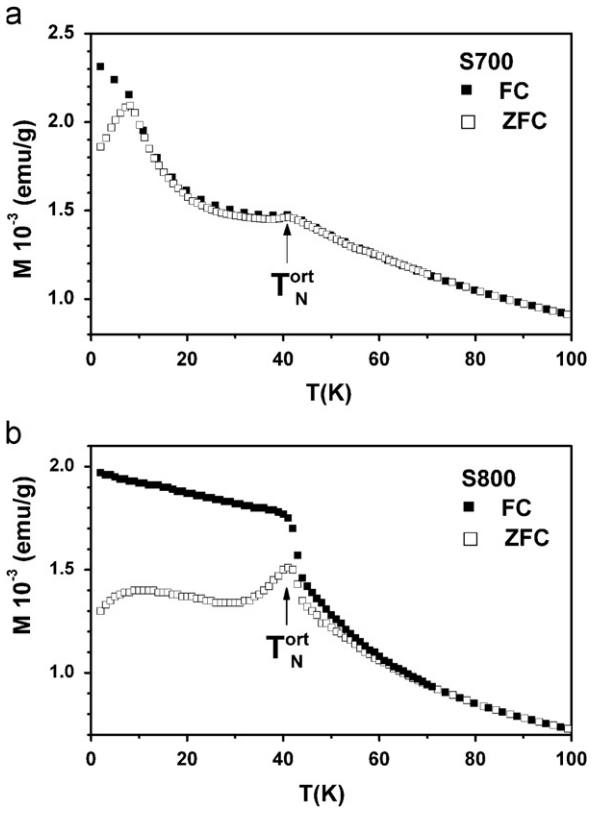

Fig. 3. Temperature dependence of magnetization in ZFC and FC regimes in an applied field of 100 Oe for samples (a) S700, and (b) S800.

maximum. In addition, magnetization in the FC branch constantly increases with the temperature decrease. Such a behavior points to a spin-glass (SG) phase of the re-entrant type, since its onset is below the temperature of the AF ordering. However, for S800 sample the low temperature peak considerably broadens while ZFC–FC separation occurs at about 70 K that is well above T_N=42 K. These results can be explained by correlating them with the conclusions drawn from XRD data. The S700 sample contains ortho-$YMnO_3$ phase only, and also its crystallinity is lower compared to the other samples that were annealed at higher temperatures. Consequently, S700 sample displays the maximum at 42 K that corresponds to AF transition point of an ortho-$YMnO_3$ phase. In addition, its low crystallinity causes structural disorder that consequently induces randomness of magnetic interaction, thus leading to the formation of SG phase with the peak at 8 K. The sample S800 is a mixture of ortho- and hexa-$YMnO_3$ phases with the improved crystallinity in comparison to the S700 sample. This results in an increase of the spin correlation lengths, and so a SG phase changes from a short-range one to a cluster-glass type which causes a broadening of the low-temperature maximum. Separation between ZFC and FC branches that occurs at about 70 K originates from the emergence of a hexa-$YMnO_3$ phase with the critical point at 70 K [26,27].

Results of magnetization measurements for S1000 and S1300 samples are shown in Fig. 4(a) and (b), respectively. Although the XRD data of the S1000 sample point to a single hexagonal phase, the existence of a peak at 42 K in ZFC branch proves that small amount of ortho-$YMnO_3$ still remains, Fig. 4(a). Also, a broad low-temperature maximum is still visible thus showing that structural defects are still present to some extent. However, in the case of S1300 sample, both peaks at 8 K and 42 K disappear, and only singularity at 71 K remains that proves phase purity of this sample. Consequently, we can conclude that annealing at 1300 °C eliminates all parasitic phases, and produces the well crystallized, pure hexagonal $YMnO_3$ phase with the AF transition point at 70 K [18,27].

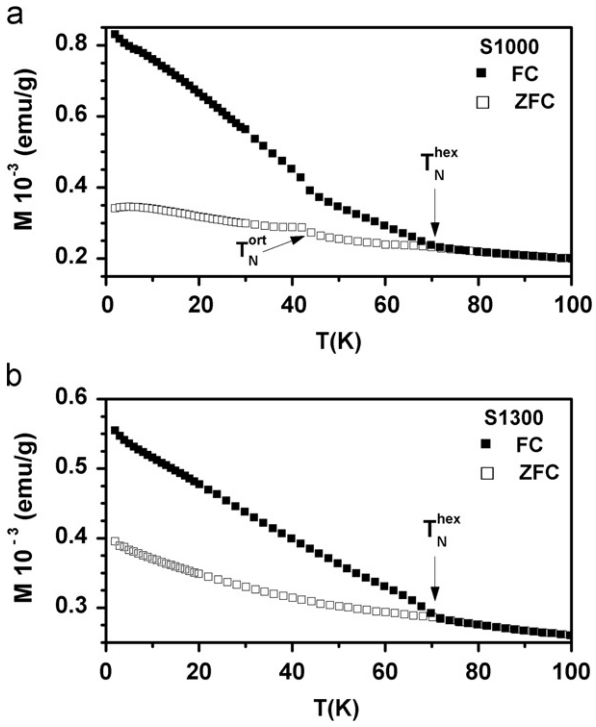

Fig. 4. Temperature dependence of magnetization in ZFC and FC regimes in an applied field of 100 Oe for samples (a) S1000, and (b) S1300.

3.3. Heat capacity

Additional probing of the phase composition of the final YMnO3 sample S1300 was done by specific heat measurements using a Quantum Design PPMS device. The temperature dependence of the measured specific heat C values is shown by open symbols in Fig. 5. Measurements were done in zero applied field, as well as in 1 kOe and 5 kOe fields, and no field dependence was noticed. The single sharp anomaly appears at 70 K for all field values, and it matches the AF transition temperature of a pure h-$YMnO_3$ phase [26] that is in excellent agreement with the magnetization measurements presented in previous section. No other anomalies were observed, which additionally speaks in favor of the phase purity of the obtained h-$YMnO_3$.

In order to verify the origin of the magnetic contribution C_{mag} to the overall heat capacity in the vicinity of 70 K we have performed a calculation of the lattice heat capacity C_{lat} and then subtracted it from the total (i.e. measured) heat capacity C. The lattice capacity C_{lat} was calculated in a manner described in Ref. [18]: two Debye functions were used, one for heavy elements (Y and Mn), and the other one for the light element (oxygen). The Debye temperatures θ_D were determined from the fit to the experimental data within the high temperature interval (160–210 K) i.e.

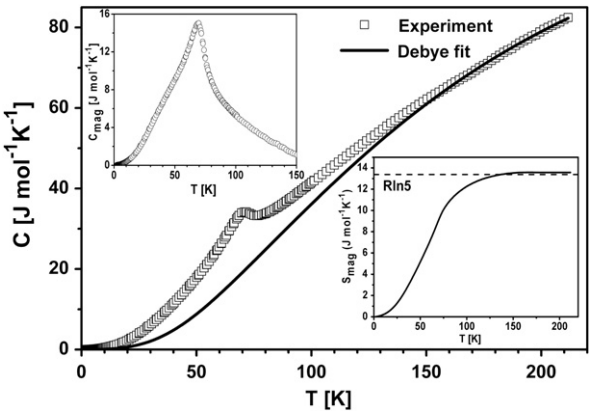

Fig. 5. Measured heat capacity (symbols) and calculated lattice heat capacity (line) by the method described in the text. Insets: magnetic contribution C_{mag} obtained by subtracting lattice contribution from the measured values (upper left); the entropy of magnetic contribution calculated by integrating C_{mag} (lower right).

for temperatures that satisfy $T > 2\ T_N$. The so-obtained values were $\theta_D(\text{heavy}) \approx 380$ K and $\theta_D(\text{light}) \approx 800$ K, which are in excellent agreement with the values from Ref. [18]. The lattice heat capacity calculated by using these Debye temperatures is depicted by full line in Fig. 5. The magnetic contribution C_{mag} is also shown in Fig. 5 (upper right inset). By integration of C_{mag}, the value of the entropy S_{mag} was obtained and it is depicted in Fig. 5 (lower right inset). The entropy value expected for Mn^{3+} ion in strong crystal field (freezing of orbital moment, thence $J=S$; $S=2$) is $S_{mag}=R\ln(2S+1)=13.38\ \text{Jmol}^{-1}\text{K}^{-1}$. Thus, a very good agreement between expected and the obtained entropy values (about 98% matching) leads to the conclusion that magnetic entropy S_{mag} originates from the $YMnO_3$ contribution only.

4. Conclusion

We have applied a new synthesis route for obtaining a single-phase hexagonal $YMnO_3$. The proposed route consists of two stages: the first one is based on the glycine–nitrate method used for obtaining an amorphous precursor powder, which was subsequently annealed during the second stage, up to the temperature of 1300 °C under the inert gas (nitrogen) flow. The process was monitored by an XRD, as well as by the magnetic and heat capacity measurements, and the analysis of these data show that precursor powder undergoes the gradual phase transformation that depends of the annealing temperature. Below 700 °C, the metastable orthorhombic phase is the first to appear, while a mixture of ortho- and hexa-phases was found to exist within the 700–900 °C range. In the temperature range 900–1000 °C, an almost complete conversion to the hexa-phase occurs but in order to obtain pure, well crystallized h-$YMnO_3$ phase, the annealing temperature of 1300 °C was necessary.

The synthesis method applied in this work has been proved to be more convenient for obtaining single-phase h-$YMnO_3$ than the usually applied solid state reaction. In addition, it is capable of producing sample free of parasitic phases that are often present in specimens obtained by other synthesis methods.

Acknowledgment

This work was supported by the Serbian Ministry of Education, Science and Technological Development (Projects III-45015 and 680-00-140/2012-09/11), and by Slovak Scientific Grant Agency (Projects SK-SRB-0054-11 and VEGA0057).

References

[1] R. von Helmolt, J. Wecker, B. Holzapfel, L. Schultz, K. Samwer, giant negative magnetoresistance in perovskite like $La_{2/3}Ba_{1/3}MnO_x$ ferromagnetic films, Physical Review Letters 71 (1993) 2331.

[2] H. Yakel, W.C. Koehler, E.F. Bertaut, F. Forrat, On the crystal structure of the Manganese (III) trioxides of the heavy lanthanides and Yttrium, Acta Crystallographica 16 (1963) 957.

[3] S.C. Abrahams, Atomic displacements at and order of all phase transitions in multiferroic $YMnO_3$ and $BaTiO_3$, Acta Crystallographica B65 (2009) 450–457.

[4] A. Seongsu Lee, Jung Hoon Pirogov, J.-G. Han, A. Park, Hoshikawa, T. Kamiyama, Direct observation of a coupling among spin, lattice, and electric dipole moment in multiferroic $YMnO_3$, Physical Review B 71 (2005) 180413.

[5] Z.J. Huang, Y. Cao, Y.Y. Sun, Y.Y. Zue, C.W Chu, Coupling between the ferroelectric and antiferromagnetic orders in $YMnO_3$, Physical Review B 56 (1997) 2623–2626.

[6] M. Janoschek, B. Roessli, S. LKeller, K NGvasaliya, Conder, E. Pomjakushina, Reduction of the ordered magnetic moment in $YMnO_3$ with hydrostatic pressure, Condensed Matter 17 (2005) 425–430.

[7] Bas B. Van Aken, Jan-Willem G. Bos, Robert A. de Groot, Thomas T.M. Palstra, Asymmetry of electron and hole doping in $YMnO_3$, Physical Review B 63 (2001) 125–127.

[8] Tapan Chatterji, Neutron scattering investigations of multiferroic $YMnO_3$, Journal of Physics 71 (2008) 847–858.

[9] A. Munoz, J.A. Alonso, M.J. Martınez-Lope, M.T. Casais, J.L. Martınez, M.T. Fernandez-D, Magnetic structure of hexagonal $RMnO_3$ (R=Y, Sc): thermal evolution from neutron powder diffraction data, Physical Review B 62 (2000) 9498–9510.

[10] Yan Ma, Yong-Jun Wu, Xiang-Ming Chen, Ji-Peng Cheng, Yi-Qi Lin, In situ synthesis of multiferroic $YMnO_3$ ceramics by SPS and their characterization, Ceramics International 35 (2009) 3051–3055.

[11] A. Munoz, J.A. Alonso, M.T. Casais, M.J. Martınez-Lope, J.L. Martınez, M.T. Fernandez-Dıaz, The magnetic structure of $YMnO_3$ perovskite revisited, Journal of Physics: Condensed Matter 14 (2002) 3285–3294.

[12] Attila Veres, Jacques G. Noudem, Stephan Fourrez, Gilles Bailleul, The influence of iron substitution to manganese on the physical properties of YMnO3, Solid State Sciences 8 (2006) 137–141.

[13] Andrew J. Overton, James L. Best, Ian Saratovsky, Michael A. Hayward, Influence of topotactic reduction on the structure and magnetism of the multiferroic YMnO3, Chemistry of Materials 21 (2009) 4940–4948.

[14] E. Bertaut, R. Pauthenet, M. Mercier, Structure magnetique de $MnYO_3$, Physics Letters 5 (1963) 27–29.

[15] W.R. Chen, F.C. Zhang, J. Miao, B. Xu, X.L. Dong, L.X. Cao, X.G. Qiu, B.R. Zhao, Pengcheng Dai, Re-entrant spin glass behavior in Mn-rich $YMnO_3$, Applied Physics Letters 87 (2005) 042508.

[16] B. Fu, Wayne Huebner, Synthesis and properties of strontium-doped yttrium manganite, Journal of Materials Research 9 (1994) 2645–2653.

[17] Bengt Hallstedt Ming Chen, J. Ludwig, Gauckler: thermodynamic assessment of the Mn–Y–O system, Journal of Alloys and Compounds 393 (2005) 114–121.

[18] D.G. Tomuta, S. Ramakrishnan, G.J. Nieuwenhuys, J.A. Mydosh, The magnetic susceptibility, specific heat and dielectric constant of hexagonal $YMnO_3$, $LuMnO_3$ and $ScMnO_3$, Journal of Physics: Condensed Matter 13 (2001) 4543–4552.

[19] G. Lescano, F.M. Figueiredo, F.M.B. Marques, J. Schmidt, Synthesis and electrical conductivity of $Y_{1-x}Mn_{1-y}O_{3-d}$, Journal of the European Ceramic Society 21 (2001) 2037–2040.

[20] M.C. Sekhar, N.V Prasad, Dielectric, Impedance, Magnetic and Magnetoelectric Measurements on $YMnO_3$, Journal of Ferroelectrics 345 (2006) 45–57.

[21] Yong Jun Yan Ma, Xiang Ming Wu, Ji Peng Chen, Yi Qi Lin Cheng, In situ synthesis of multiferroic $YMnO_3$ ceramics by SPS and their characterization, Ceramics International 35 (2009) 3051–3055.

[22] K. Dwight, N. Menyuk, Magnetic properties of Mn_3O_4 and the canted spin problem, Physical Review 119 (1960) 1470–1479.

[23] C Ma, J-Q Yan, K W Dennis, A Llobet, R W McCallum, X Tan, Effect of oxygen content on the magnetic properties of multiferroic $YMn_{(2)}O_{(5+\delta)}$, Journal of Physics: Condensed Matter 21 (2009) 346002.

[24] A. Munoz, J.A. Alonso, M.T. Casais, M.J. Martinez-Lope, J.L. Martinez, M.T. Fernandez-Diaz, The magnetic structure of $YMnO_3$ perovskite revisited, Journal of Physics: Condensed Matter 14 (2002) 3285–3294.

[25] B. Lorenz, Y.Q. Wang, Y.Y. Sun, C.W. Chu, Large magnetodielectric effects in orthorhombic $HoMnO_3$ and $YMnO_3$, Physical Review B 70 (2004) 212412.

[26] U. Adem, A.A. Nugroho, A. Meetsma, T.T.M. Palstra, Ferroelectric displacements in multiferroic $Y(Mn,Ga)O_3$, Physical Review B 75 (2007) 14108.

[27] Hiroshi Kristin Bergum, Helmer Okamoto, Tor Fjellvag, Mari-Ann Grande, Einarsrud and Sverre M. Sellbach: Synthesis, structure and magnetic properties of nanocrystalline $YMnO_3$, Dalton Transactions 40 (2011) 7583.